

Published in final edited form as:

Nat Cell Biol. 2013 August ; 15(8): 905–915. doi:10.1038/ncb2798.

A tripartite transcription factor network regulates primordial germ cell specification in mice

Erna Magnúsdóttir^{1,2,7}, Sabine Dietmann³, Kazuhiro Murakami^{1,2}, Ufuk Günesdogan^{1,2}, Fuchou Tang^{1,2,6}, Siqin Bao^{1,2}, Evangelia Diamanti⁴, Kaiqin Lao⁵, Bertie Gottgens⁴, and M. Azim Surani^{1,2,3,*}

¹Wellcome Trust/Cancer Research UK Gurdon Institute, University of Cambridge, Tennis Court Road, Cambridge CB2 1QN, United Kingdom

²Department of Physiology, Development and Neuroscience, University of Cambridge, Downing Street, Cambridge CB2 3DY, United Kingdom

³Wellcome Trust-Medical Research Council Stem Cell Institute, University of Cambridge, Tennis Court Road, Cambridge CB2 1QN, United Kingdom

⁴Cambridge Institute for Medical Research, Wellcome Trust–MRC Building, Hills Road, Cambridge CB2 0XY, United Kingdom

⁵Genetic Systems, Applied Biosystems, Part of Life Technologies, 850 Lincoln Centre Drive, Foster City, CA 94404, USA

Abstract

Transitions in cell states are controlled by combinatorial actions of transcription factors. For primordial germ cell (PGC) specification, BLIMP1 the key regulator apparently acts together with PRDM14 and AP2. To investigate their individual and combinatorial functions, we first sought an *in vitro* system for transcriptional readouts and ChIPseq analysis. We then integrated this data with information from single cell transcriptome analysis of normal and mutant PGCs. Here we show that BLIMP1 binds directly to repress somatic and cell proliferation genes. It also directly induces AP2, which together with PRDM14 initiates the PGC-specific fate. We determined the occupancy of critical genes by AP2, which when computed altogether with those with BLIMP1 and PRDM14, individually and cooperatively, reveals a tripartite mutually interdependent transcriptional network for PGCs. We also demonstrate that in principle, BLIMP1, AP2 and PRDM14 are sufficient for PGC specification, and the unprecedented resetting of the epigenome towards a basal state.

Primordial germ cells (PGCs) in mice originate from the rapidly dividing post implantation epiblast cells that are primed for somatic fate, following repression of some pluripotency genes¹. They also exhibit an inactive X chromosome, histone H3 lysine nine dimethylation (H3K9me2) and DNA methylation^{2,3}. A transcriptional network for PGC specification should reverse this trend by the time 30-40 founder PGCs are established at embryonic day 7.5 (E7.5).

PGC fate is initiated by BMP4-induced expression of BLIMP1 in a few proximal epiblast cells at E6.25⁴⁻⁸, which marks their divergence from somatic neighbours (see Fig 3b).

*Correspondence: a.surani@gurdon.cam.ac.uk.

⁶Current Address: College of Life Sciences, Peking University, 5 Yiheyuan Road, Beijing, 100871, China

⁷Current Address: Department of Biochemistry and Molecular Biology, University of Iceland, Vatnsmyrarveggi 16, 101 Reykjavík, Iceland.

Indeed, BLIMP1 mutant cells fail as PGCs and resemble neighbouring somatic cells^{7,9–11}. BLIMP1 binds to a specific DNA sequence^{12–20} to either repress^{21–25} or activate²⁶ its direct targets. Shortly after BLIMP1, there is induction of *Prdm14* also by BMP4²⁷, followed by *Tcfap2c* encoding AP2²⁸ (see Fig 3b). Genetic experiments indicate that these factors are individually critical for PGC specification. It is important however to establish if their combinatorial roles and precise targets are necessary and sufficient for PGC specification, and for the initiation of the unique epigenetic program²⁹.

In this study we combined information from different experimental models to establish how BLIMP1, PRDM14 and AP2 contribute to PGC specification, both individually and combinatorially. We propose a tripartite transcriptional network that accounts for PGC specification and their unique properties. Indeed, co-expression of BLIMP1, AP2 and PRDM14 in an *in vitro* model can substitute for cytokines in the direct induction of PGC-like cells (PGCLCs). Close scrutiny of the genetic network also provides a detailed view of how these genetic factors regulate the unique epigenetic program in germ cells, which might serve as a paradigm for wider applications in the context of tissue regeneration and experimental manipulation of cell fates.

RESULTS

We first sought an *in vitro* surrogate cell-culture system to examine the individual and cooperative roles of BLIMP1, PRDM14 and AP2, and to identify their direct targets by chromatin immunoprecipitation (ChIP) experiments, which requires large amounts of material. This is difficult with PGCs since they are relatively rare, difficult to culture, transfect and manipulate. We therefore tested BLIMP1 expression in several primary cell types, embryonic stem cells (mESCs), embryonic germ cells (EGCs) and epiblast stem cells (EpiSC), but none of them survived except for P19 embryonal carcinoma cells (P19EC)²⁹ (Fig 1a). Indeed, P19EC cells are also appropriate for this purpose because they originate from E7.5 epiblast³⁰, and share important properties of post implantation epiblast, the precursors of PGCs *in vivo*^{31,32}.

Repression of somatic program and induction of PGC genes in P19EC cells

We examined P19EC cells for transcriptional response following ectopic expression of BLIMP1-EGFP fusion protein or EGFP alone after 24h with low (24h-LO) and high expression (24h-HI), and all fluorescent cells at 48h (Fig. S1a). Whereas the 24h-HI cells showed an apoptosis response due to a strong dose dependent effect³³, this was not the case with 24h-LO cells. We therefore focused mainly on 24h-LO and 48h cells (Fig S1b, Fig S2).

BLIMP1 in P19EC cells induced gene repression including mesendodermal factor *Eomes*, *HoxA5*, *Evx1*, *Myc*, and of *de novo* DNA methyltransferase, *Dnmt3b* (Fig S1b), which are amongst the key responses observed in PGCs^{2,34}. Importantly, PGC genes, *Nanos3*, and *Rhox9* were induced. By lowering the statistical threshold to FDR = 0.05, we detected an induction of *Dppa3/Stella*, and *Tcfap2c* (encoding AP2), (Fig S1b, 1b, Table S1). Furthermore, RT-qPCR revealed an induction of *Dnd1* and *Prdm14* at 48h, and PGC markers, *Dazl* and *Ddx4* (Fig. 1b). While *Oct4/Pou5f1* expression continued (Table S1), we noted repression of *Nanog*, which could explain the induction of *Gata4* and *FoxQ1*³⁵ (Fig S1b and Table S1). Overall and in important respects, the response of P19EC to BLIMP1 approximates that seen during PGC specification *in vivo*.

We then looked at the effects of all three factors in P19EC cells following stable expression of PRDM14 and AP2, both individually and together. We transfected control cells and the stable lines with BLIMP1-EGFP or EGFP alone for 24 hours and examined sorted fluorescent cells. This showed repression of *Eomes* and *T-Brachyury*, while PRDM14 alone

suppressed *Dnmt3b* (Fig 1c), its direct target³⁶. While BLIMP1 repressed *Myc*, PRDM14 in combination with AP2 modestly induced *Myc* expression, an effect that was overcome by BLIMP1 expression. Thus, repression of somatic regulators is complex, and may not be attributable to BLIMP1 alone.

The induction of PGC genes revealed co-operative effects of AP2 and PRDM14, which induced *Nanos3* and *Prdm1* (encoding BLIMP1), with a modest induction of *Ddx4*. While *Nanos3* induction was attenuated by BLIMP1, *Dnd1* was induced by 15-fold when all three factors were present, but *Dppa3* was strictly PRDM14-dependent (Fig 1c). These observations show that PRDM14 and AP2 cooperatively induce the germ cell programme, with the additional effect of BLIMP1 on *Dnd1* induction.

The analysis of P19ECs shows a response to BLIMP1, PRDM14 and AP2 individually and collectively, with features that are pertinent to PGCs, including the repression of somatic genes and induction of PGC genes. We posit that P19EC cells are appropriate for the identification of direct targets of the three key determinants of PGC specification.

Identification of BLIMP1 targets and their relevance for PGC specification

To identify BLIMP1 targets, we transfected P19ECs with BLIMP1-EGFP, followed by ChIP sequencing (ChIPseq) using an EGFP antibody. This revealed 5046 BLIMP1 high-confidence binding peaks for 4389 protein coding and 313 non-coding genes (Table S2 and S3), including 8/11 known targets such as *Myc* and *Id3* (Fig 2a). We observed a peak distribution with a median position of +171.5 bp relative to transcriptional start sites (TSS) (Fig. 2b,c) consistent with BLIMP1 binding on promoters and an enrichment of the previously characterized consensus binding sequence for BLIMP1³⁷ (p-value = 1.1×10^{-388}) (Fig. 2d). Notably, BLIMP1 bound to *T-Brachyury*, *Eomes* and the entire *Hox* gene loci (Fig. 2e and Table S3) reflecting its role in PGC specification *in vivo*^{7,9}. Functional category analysis revealed a striking enrichment of BLIMP1 binding to genes encoding transcriptional regulators and of genes regulating developmental processes (Fig 2f). Moreover, BLIMP1 was bound to *Tcfap2c* (encoding AP2), which is induced in PGCs (see later).

We validated *Myc* and several novel BLIMP1 bound regions by ChIP-qPCR in P19ECs (Fig 2g). We also validated BLIMP1 binding to *Eomes*, *Dnmt3b*, *HoxB2* and *Myc* in PGC-like cells (PGCLCs) generated *in vitro*³⁸ with a ChIP grade BLIMP1 antibody³⁷ (Fig 2h), but comprehensive analysis in PGCLCs was technically not feasible owing to limited amounts of precipitated DNA that could be generated.

To determine the significance of BLIMP1 targets, we scrutinised transcriptional changes in wild type and *Prdm1* (BLIMP1) mutant PGCs from E6.25-E8.5 embryos, including E7.5 somatic neighbours, which share a common ancestry (Fig 3a). For this, we performed single-cell RNA-Seq analysis and found that all three factors; *Prdm1* (encoding BLIMP1), *Tcfap2c* (encoding AP2), and *Prdm14* were fully induced by E6.5 in putative PGCs, with extensive repression of somatic and cell cycle regulators, and induction of the PGC program^{7,2} (Fig 3b,c, S3a,b, Table S4). By contrast, we detected expression of somatic genes and a lack of expression of some germ cell genes in *Prdm1* mutant cells (Fig 3b,c). Overall, the E7.5 single cell expression profiles of *Prdm1* mutant cells clustered with E7.5 somatic cells and not with PGCs (Fig 3a).

We then carried out a global assessment of BLIMP1 bound genes in relation to the differentially expressed genes in PGCs (compared to the binding to the whole set of expressed genes). Indeed, BLIMP1 was bound to both repressed (*Brachyury* and *Dnmt3b*), and induced (*Cbx7*) genes. Notably, BLIMP1 bound to *Tcfap2c* (encoding AP2), which is

induced (Fig. 3c,d and see below). We calculated the binding scores for reads both inside and outside of peak regions and their distance to promoters (see methods), as well as the defined peak regions. This revealed that the repressed genes in E7.5-E8.5 PGCs compared to either somatic cells or *Prdm1* (BLIMP1) mutant cells, are enriched for BLIMP1 (Fig 4a). The repressed genes that were bound by BLIMP1 had a greater enrichment for developmental, transcriptional and Wnt-signalling function compared to the whole set of repressed genes (Fig S3a). Since misregulated gene expression in the *Prdm1* mutant cells from *in vivo* is a direct consequence of the lack of BLIMP1 in these cells, this result further shows the functional relevance of our analysis to the processes occurring during PGC specification *in vivo*.

Comparing the ChIPseq data with the BLIMP1-induced changes in P19ECs revealed a predominant effect on repression of direct targets. Whereas BLIMP1 bound with 24.1% of the genes in the genome (Fig. 4b, Whole Array), nearly 50% of the repressed genes were bound by BLIMP1, but binding to induced genes was close to background (Fig.4b). We further observed a striking enrichment of BLIMP1 binding on repressed genes in both P19ECs as well as in E7.5 PGCs compared to soma (Fig 4c and S3e) where 34/59 repressed genes were bound by BLIMP1. This is statistically a very high over-representation, (chi-square p-value = 1.8×10^{-10}), which shows conclusively that the dominant effect of BLIMP1 in PGC specification is gene repression, including those required for the somatic fate.

AP2γ binds to germ cell genes and somatic regulators

Toward building a genetic network for PGC specification, we performed an unbiased scan of the BLIMP1 binding regions for transcription factor binding motifs (Fig. S4a). We found a bimodal distribution of AP2 family motifs surrounding the BLIMP1 peak (Fig S4b). Similarly, PRDM14 binding sites were also highly enriched for AP2 motifs³⁶ (Fig. S4c,d). We therefore mapped PRDM14 and BLIMP1 binding sites to all the genes in the PGC transcriptome, and then found AP2 motifs within the binding regions³⁹⁻⁴¹. This revealed a preferential enrichment of genes regulated during PGC specification that were associated with BLIMP1 and PRDM14 binding sites that contained AP2 motifs (Fig S4e). This strongly implies that the three factors cooperate both in gene induction and repression in PGCs. This prompted us to carry out ChIPseq analysis for AP2 .

With P19ECs stably expressing AP2 , we performed ChIPseq with a previously validated antibody⁴¹, and identified 3191 high confidence AP2 binding regions that map to 1393 genes (Table S5 and S6). The peaks were enriched with the AP2 consensus motif (Fig 5a) (p-value = 1.1×10^{-241}). AP2 binding was centred on promoters at a median position of -53bp relative to TSS, albeit the peak distribution was much broader than that of BLIMP1 (Fig 5b), perhaps implying binding to gene-distal sequence elements. Importantly, the *Pou5f1* distal enhancer which is bound by PRDM14 and pluripotency transcription factors, was amongst the most strongly bound regions (Fig 5c)^{36,42,43}. Notably, *Pou5f1* expression in the post implantation epiblast and P19ECs is driven from the proximal enhancer, while the distal enhancer is utilised following PGC specification. Several somatic genes were also bound by AP2 , including *Hoxa11*, *HoxB13* and *T-Brachyury*, and regions distal to the TSS of *Nanos3* and the first intron of *Dppa3* (Fig 5c, d, Table S6).

Analysis of functional categories of targets revealed highly significant binding to PGC genes (e.g. *Nanog*, *Dppa3* and *Pou5f1*), and E6.0 epiblast (e.g. Activin and FGF receptor genes *Acvr1b*, *Fgfr1* and *Fgfr2*). This is consistent with AP2 being involved in PGC specification from epiblast cells (Fig 5e,f Table S6). Furthermore, AP2 was enriched for genes involved in morphogenesis and development, indicating a relevance to PGCs and somatic gene repression.

Transcriptional network for PGC specification

Next, we combined all available information for a detailed scrutiny of how the key regulators induce PGCs. With respect to gene expression in PGCs versus soma at E7.5, AP2 was significantly enriched on both induced and repressed genes (Fig 6a), as confirmed by the hypergeometric distribution statistical test (Fig 6b). The repressed genes were also co-bound by BLIMP1-AP2, and by PRDM14-AP2, and co-binding of all three factors showed enhanced enrichment with increased degree of repression (Fig 6a, left panel), more so than with either PRDM14 or BLIMP1 alone. By contrast, the induced genes were preferentially enriched for PRDM14 and AP2 together (Fig 6a,b right panels), where the enrichment of BLIMP1 alone or in combinations was statistically not significant (Fig 6b). While AP2 clearly has a significant impact on gene expression genes bound by AP2 alone were depleted of association with specific functional gene categories (Fig S5,6), unless co-bound by BLIMP1 and/or PRDM14. Hence, co-binding of BLIMP1 with the other factors mediates repression, whereas AP2 and PRDM14 co-binding leads to gene induction, suggesting a high degree of co-regulation by these factors. Statistical testing of the overlap of binding sites for the three factors ($p < 0.0001$ permutation test) (Fig 6c and S8a) and the overlap of genes bound by the three factors ($p < 1 \times 10^{-299}$, chi-square test) (Fig 6d and S8b) further indicates an enrichment of co-bound genes over what would be expected by random chance, further supporting the functional relationship between the three factors.

BLIMP1, AP2 and PRDM14 co-binding on repressed genes included developmental and signalling genes, particularly those of Fgf and Wnt signalling. BLIMP1 was preferentially bound to proliferation genes, and PRDM14 and AP2 to cell-motility and cytoskeleton organization genes (Fig S5a,S6a), indicating initiation of PGC migration. All three factors are over-represented on induced genes involved in actin cytoskeleton organization and intracellular signalling cascades (Fig S5b,S6b), although PRDM14, either alone or with AP2, is predominant over BLIMP1. Critically, PRDM14 binds to PGC specific genes, including *Tcfap2c* (encoding AP2), *Sox2* and *Kit* as well as *Dnd1*, *Nanos3*, *Dppa3*, *Prdm1* (encoding BLIMP1) and *Prdm14* (Fig 6e, S6b). Furthermore, AP2 binds to *Dppa3* as well as *Nanos3*, and acts cooperatively with PRDM14 in the induction of *Nanos3* (Fig 1c, 6e and S6b). All three factors are involved in the induction of *Dnd1* (Fig 1c). Thus, after the induction of AP2 by BLIMP1, it cooperates with PRDM14 to induce PGC genes.

In the context of a compendium of transcription factors in mESCs⁴⁴, BLIMP1 clustered predominantly with self-renewal and polycomb factors, consistent with somatic gene repression (Fig 7 and S7). PRDM14 clustered with pluripotency transcription factors, but AP2 associated weakly with factors in the compendium (Fig S7). This underlines the context-dependent combinatorial action of these three factors, which as expected is not fully captured in comparison to mESCs factors.

A key role of the transcriptional network is in initiating epigenetic reprogramming in PGCs. Consistently, BLIMP1 and PRDM14 repress *Kdm6b* encoding a H3K27 demethylase, while PRDM14 mediates the induction of the H3K9 demethylase *Kdm4b*, and together with BLIMP1, induces *Kdm3a* (Fig S5a,b). This ensures the erasure of H3K9me2 that is prerequisite for global DNA demethylation⁴⁵. The two factors also repress *de novo* DNA methyltransferase, *Dnmt3b* as well as *Uhrf1*, encoding an accessory protein for the maintenance DNA methyltransferase, DNMT1; this facilitates global DNA demethylation in PGCs (Fig S6a). BLIMP1 and PRDM14 each bind to one of the two promoters to repress *Uhrf1* in PGCs (Fig 6e), while PRDM14 alone in mESC is insufficient to do so⁴⁶. The regulation of histone- and DNA methylases links PGC specification to the dynamic and genome wide epigenetic reprogramming⁴⁷. BLIMP1 and PRDM14 bind extensively to differentially expressed genes during PGC specification, while AP2 binds to a subset of

them and perhaps acts as a facilitator of key events, except perhaps for chromatin modifications

The proposed transcriptional network is interdependent, since *Tcfap2c* (encoding AP2) expression is dependent on BLIMP1. Expression of *Prdm14* and *Prdm1* (encoding BLIMP1) expression is mutually interdependent as revealed by genetic experiments^{7,27}. PRDM14 also binds *Tcfap2c* and could enhance *Tcfap2c* expression after its induction by BLIMP1. This supports an obligatory functional relationship between BLIMP1, PRDM14 and AP2 as critical regulators of PGC specification.

Direct induction of PGC-like fate by BLIMP1, AP2 γ and PRDM14 *in vitro*

Next we asked whether BLIMP1, AP2 and PRDM14 are sufficient to directly induce PGC fate and used the *in vitro* induction of PGCLCs to test this premise²⁹. PGCLCs can be induced in response to cytokines (Fig 8a, left panel), which we observed in 47.4-52.6% of the cells after 4 days. Using the same reporter cells harbouring doxycycline inducible constructs for the three transcription factors, we observed induction of PGCLCs in the absence of cytokines in ~45-60% of the cells (Fig 8a, right panel). Both the overall response and transcriptional analysis by qPCR using the sorted fluorescent PGCLCs were remarkably similar to those induced by cytokines with respect to the key PGC, epigenetic and somatic cell regulators. The response to the transcription factors was slightly enhanced, (Fig 8b and 8c) as reflected in the higher induction of *Dppa3* and *Nanos3*, and a more pronounced repression of *HoxB1* and *T-Brachyury*. This observation establishes the principle that the proposed transcriptional network delineating specific and combined functions of BLIMP1, AP2 and PRDM14 accounts for the necessary gene expression changes for PGC specification. Further work in the future will advance our knowledge of how these factors, both individually and in combination, induce PGC fate.

DISCUSSION

We present a comprehensive examination of the initiation of PGC specification by the combinatorial roles of BLIMP1, AP2 and PRDM14, leading to a unique epigenetic program culminating in the epigenetic basal state^{48,49}. Co-expression of the three factors is by itself apparently sufficient to induce PGC-like fate in the absence of cytokines, and supports the proposed tripartite genetic network for PGC specification.

BLIMP1, PRDM14 and AP2 contribute to the repression of mesodermal genes in PGCs to set them apart from their somatic neighbours; until then, these cells are indistinguishable from each other. BLIMP1 has a dominant function in this respect, which is reinforced by PRDM14 and AP2. By contrast, PRDM14 and AP2 together are associated with gene induction. Notably, *Tcfap2c* (encoding AP2) is a direct target of BLIMP1 and induced by it in P19EC cells *in vitro*, and probably maintained thereafter by PRDM14 in PGCs. *Tcfap2c* fails to be induced in BLIMP1 mutant PGC-like cells *in vivo* and its induction by BLIMP1 is perhaps the vital link for the initiation of the PGC-specific genes.

The high overlap of AP2 targets with that of BLIMP1 and PRDM14 implies that it cooperates, augments or otherwise modulates the response of a subset of the targets. Furthermore, the distinct and predominant binding of BLIMP1 to promoter regions as opposed to gene-distal regulatory regions binding noted for PRDM14⁵⁰, suggests parallel mechanisms in regulating transcription. The collaborative role of AP2 is also reflected in its broad distribution that is centred on promoters, but potentially, encompasses distal elements.

This comprehensive insight on PGC specification in mice, may facilitate investigations on germ cells in other mammals, including humans, and enhance an understanding of context dependent functions of transcription factors. For example, AP2 has a role in trophoblast differentiation in conjunction with CDX2 and EOMES, whereas it participates in the repression of *Eomes* in PGCs. BLIMP1 also drives cell fate commitment in several different lineages, while PRDM14 is crucial for pluripotency in ES cells^{50–52}. These differences are presumably linked to the molecular control of competence, which precedes and ‘anticipates’ specific cell fate decisions.

A fundamental property of early germ cells are the unique epigenetic changes that ensue following PGC specification, leading to global erasure of DNA methylation and acquisition of a basal epigenetic state. The mechanism that regulates this unique resetting of the epigenome in germ cells could in principle be extended towards approaches for modifying epigenetic states of normal and diseased tissues. This study may help towards achieving wider objects of general interest in the field of regenerative medicine.

Supplementary Material

Refer to Web version on PubMed Central for supplementary material.

Acknowledgments

We thank Nigel Miller for flow-cytometry, and Matthew Trotter, Charles Bradshaw and George Allen for bioinformatics analysis. We thank Roopsha Sengupta and Jamie Hackett for critically reading the manuscript. This work was supported by grants from the Wellcome Trust and HFSP to M.A.S and the ERC to E.M.

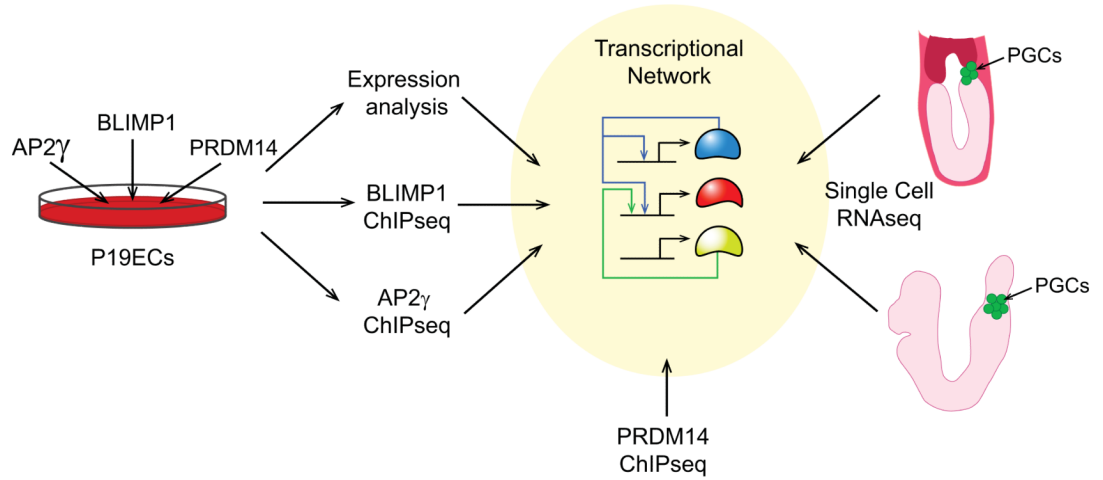
REFERENCES

1. Fuhrmann G, et al. Mouse germline restriction of Oct4 expression by germ cell nuclear factor. *Dev Cell*. 2001; 1:377–387. [PubMed: 11702949]
2. Seki Y, et al. Extensive and orderly reprogramming of genome-wide chromatin modifications associated with specification and early development of germ cells in mice. *Developmental Biology*. 2005; 278:440–458. [PubMed: 15680362]
3. Borgel J, et al. Targets and dynamics of promoter DNA methylation during early mouse development. *Nature genetics*. 2010; 42:1093–100. [PubMed: 21057502]
4. McLaren A, Lawson KA. How is the mouse germ-cell lineage established? *Differentiation; research in biological diversity*. 2005; 73:435–7.
5. Saitou M, Barton SC, Surani MA. A molecular programme for the specification of germ cell fate in mice. *Nature*. 2002; 418:293–300. [PubMed: 12124616]
6. Yamaji M, et al. Critical function of Prdm14 for the establishment of the germ cell lineage in mice. *Nat Genet*. 2008; 40:1016–1022. [PubMed: 18622394]
7. Kurimoto K, et al. Complex genome-wide transcription dynamics orchestrated by Blimp1 for the specification of the germ cell lineage in mice. *Genes & development*. 2008; 22:1617–35. [PubMed: 18559478]
8. Robertson EJ, et al. Blimp1 regulates development of the posterior forelimb, caudal pharyngeal arches, heart and sensory vibrissae in mice. *Development (Cambridge, England)*. 2007; 134:4335–45.
9. Ohinata Y, et al. Blimp1 is a critical determinant of the germ cell lineage in mice. *Nature*. 2005; 436:207–213. [PubMed: 15937476]
10. Vincent SD, et al. The zinc finger transcriptional repressor Blimp1/Prdm1 is dispensable for early axis formation but is required for specification of primordial germ cells in the mouse. *Development (Cambridge, England)*. 2005; 132:1315–25.
11. Saitou M, Payer B, O’Carroll D, Ohinata Y, Surani MA. Blimp1 and the emergence of the germ line during development in the mouse. *Cell Cycle*. 2005; 4:1736–1740. [PubMed: 16294024]

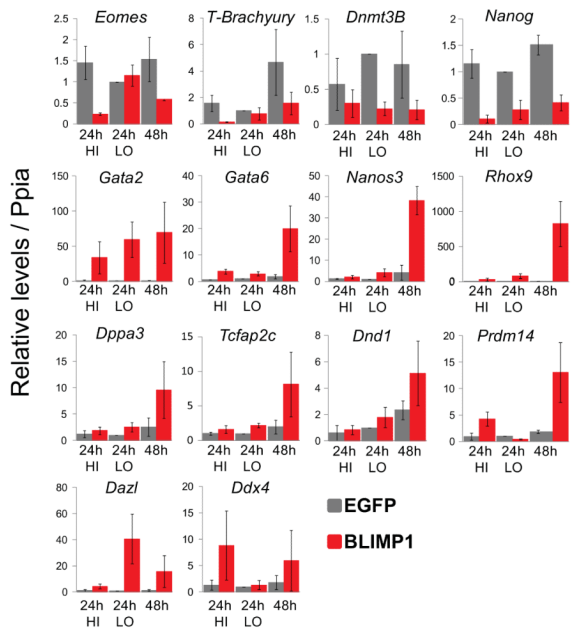
12. Turner CA, Mack DH, Davis MM. Blimp-1, a novel zinc finger-containing protein that can drive the maturation of B lymphocytes into immunoglobulin-secreting cells. *Cell*. 1994; 77:297–306. [PubMed: 8168136]
13. Keller AD, Maniatis T. Identification and characterization of a novel repressor of beta-interferon gene expression. *Genes & Development*. 1991; 5:868–879. [PubMed: 1851123]
14. Morgan, M. a J., et al. Blimp-1/Prdm1 alternative promoter usage during mouse development and plasma cell differentiation. *Molecular and cellular biology*. 2009; 29:5813–27. [PubMed: 19737919]
15. Martins GA, et al. Transcriptional repressor Blimp-1 regulates T cell homeostasis and function. *Nature immunology*. 2006; 7:457–65. [PubMed: 16565721]
16. Kallies A, et al. Transcriptional repressor Blimp-1 is essential for T cell homeostasis and self-tolerance. *Nature immunology*. 2006; 7:466–74. [PubMed: 16565720]
17. Chan Y-H, et al. Absence of the transcriptional repressor Blimp-1 in hematopoietic lineages reveals its role in dendritic cell homeostatic development and function. *Journal of immunology* (Baltimore, Md. : 1950). 2009; 183:7039–46.
18. Nishikawa K, et al. Blimp1-mediated repression of negative regulators is required for osteoclast differentiation. *Proceedings of the National Academy of Sciences of the United States of America*. 2010; 107:3117–22. [PubMed: 20133620]
19. Chang DH, Angelin-Duclos C, Calame K. BLIMP-1: trigger for differentiation of myeloid lineage. *Nature immunology*. 2000; 1:169–76. [PubMed: 11248811]
20. Kim SJ, Zou YR, Goldstein J, Reizis B, Diamond B. Tolerogenic function of Blimp-1 in dendritic cells. *The Journal of experimental medicine*. 2011; 208:2193–2199. [PubMed: 21948081]
21. Yu J, Angelin-Duclos C, Greenwood J, Liao J, Calame K. Transcriptional Repression by Blimp-1 (PRDI-BF1) Involves Recruitment of Histone Deacetylase. *Molecular and Cellular Biology*. 2000; 20:2592–2603. [PubMed: 10713181]
22. Ren B, Chee KJ, Kim TH, Maniatis T. PRDI-BF1/Blimp-1 repression is mediated by corepressors of the Groucho family of proteins. *Genes & Development*. 1999; 13:125–137. [PubMed: 9887105]
23. Gyory I, Wu J, Fejér G, Seto E, Wright KL. PRDI-BF1 recruits the histone H3 methyltransferase G9a in transcriptional silencing. *Nature immunology*. 2004; 5:299–308. [PubMed: 14985713]
24. Ancelin K, et al. Blimp1 associates with Prmt5 and directs histone arginine methylation in mouse germ cells. *Nat Cell Biol*. 2006; 8:623–630. [PubMed: 16699504]
25. Su S-T, et al. Involvement of histone demethylase LSD1 in Blimp-1-mediated gene repression during plasma cell differentiation. *Molecular and cellular biology*. 2009; 29:1421–31. [PubMed: 19124609]
26. Cretney E, et al. The transcription factors Blimp-1 and IRF4 jointly control the differentiation and function of effector regulatory T cells. *Nat Immunol*. 2011; 12:304–311. [PubMed: 21378976]
27. Yamaji M, et al. Critical function of Prdm14 for the establishment of the germ cell lineage in mice. *Nature Genetics*. 2008; 40:1016–1022. [PubMed: 18622394]
28. Weber S, et al. Critical function of AP-2 gamma/TCFAP2C in mouse embryonic germ cell maintenance. *Biology of reproduction*. 2010; 82:214–23. [PubMed: 19776388]
29. Hackett, J. a; Zylitz, JJ.; Surani, MA. Parallel mechanisms of epigenetic reprogramming in the germline. *Trends in genetics : TIG* 1–11. 2012 doi:10.1016/j.tig.2012.01.005.
30. MCBURNEY M. Isolation of male embryonal carcinoma cells and their chromosome replication patterns*1. *Developmental Biology*. 1982; 89:503–508. [PubMed: 7056443]
31. Yeom YI, et al. Germline regulatory element of Oct-4 specific for the totipotent cycle of embryonal cells. *Development (Cambridge, England)*. 1996; 122:881–94.
32. Chambers I, et al. Functional Expression Cloning of Nanog, a Pluripotency Sustaining Factor in Embryonic Stem Cells. *Cell*. 2003; 113:643–655. [PubMed: 12787505]
33. Ancelin K, et al. Blimp1 associates with Prmt5 and directs histone arginine methylation in mouse germ cells. *Nat Cell Biol*. 2006; 8:623–630. [PubMed: 16699504]
34. Yabuta Y, Kurimoto K, Ohinata Y, Seki Y, Saitou M. Gene Expression Dynamics During Germline Specification in Mice Identified by Quantitative Single-Cell Gene Expression Profiling. *Biol Reprod*. 2006; 75:705–716. [PubMed: 16870942]

35. Mitsui K, et al. The homeoprotein Nanog is required for maintenance of pluripotency in mouse epiblast and ES cells. *Cell*. 2003; 113:631–42. [PubMed: 12787504]
36. Ma Z, Swigut T, Valouev A, Rada-Iglesias A, Wysocka J. Sequence-specific regulator Prdm14 safeguards mouse ESCs from entering extraembryonic endoderm fates. *Nature structural & molecular biology*. 2011; 18:120–7.
37. Kuo TC, Calame KL. B lymphocyte-induced maturation protein (Blimp)-1, IFN regulatory factor (IRF)-1, and IRF-2 can bind to the same regulatory sites. *J Immunol*. 2004; 173:5556–5563. [PubMed: 15494505]
38. Hayashi K, Ohta H, Kurimoto K, Aramaki S, Saitou M. Reconstitution of the mouse germ cell specification pathway in culture by pluripotent stem cells. *Cell*. 2011; 146:519–32. [PubMed: 21820164]
39. Woodfield GW, Chen Y, Bair TB, Domann FE, Weigel RJ. Identification of Primary Gene Targets of TFAP2C in Hormone Responsive Breast Carcinoma Cells. 2010; 962:948–962.
40. Tan SK, et al. AP-2 regulates oestrogen receptor-mediated long-range chromatin interaction and gene transcription. *The EMBO journal*. 2011; 30:2569–81. [PubMed: 21572391]
41. Kidder BL, Palmer S. Examination of transcriptional networks reveals an important role for TCFAP2C, SMARCA4, and EOMES in trophoblast stem cell maintenance. *Genome research*. 2010; 20:458–72. [PubMed: 20176728]
42. Loh YH, et al. The Oct4 and Nanog transcription network regulates pluripotency in mouse embryonic stem cells. *Nat Genet*. 2006; 38:431–440. [PubMed: 16518401]
43. Chen X, et al. Integration of external signaling pathways with the core transcriptional network in embryonic stem cells. *Cell*. 2008; 133:1106–17. [PubMed: 18555785]
44. Sugimoto, Toshimi; Diamanti, Evangelia; Joshi, Anagha; Hannah, Rebecca; Ohtsuka, Satoshi; Göttgens, Berthold; Niwa, Hitoshi; Smith, Austin. G. M. ESRRB is a pivotal target of the GSK3 / Tcf3 axis regulating embryonic stem cell self-renewal. *Cell Stem Cell*. 2012
45. Nakamura T, et al. PGC7 binds histone H3K9me2 to protect against conversion of 5mC to 5hmC in early embryos. *Nature*. 2012:2–7. doi:10.1038/nature11093.
46. Grabole, Nils; Tischler, Julia; Leitch, Harry; Hackett, Jamie; Kim, Shinseog; Tang, Fuchou; Magnúsdóttir, Erna. A. S. Prdm14 promotes germline fate and naïve pluripotency by modulating signalling and the epigenome. *EMBO Reports*. 2013 In Press.
47. Hajkova P, et al. Epigenetic reprogramming in mouse primordial germ cells. *Mech Dev*. 2002; 117:15–23. [PubMed: 12204247]
48. Hajkova P, et al. Epigenetic reprogramming in mouse primordial germ cells. *Mech Dev*. 2002; 117:15–23. [PubMed: 12204247]
49. Hajkova P, et al. Chromatin dynamics during epigenetic reprogramming in the mouse germ line. *Nature*. 2008; 452:877–881. [PubMed: 18354397]
50. Ma Z, Swigut T, Valouev A, Rada-Iglesias A, Wysocka J. Sequence-specific regulator Prdm14 safeguards mouse ESCs from entering extraembryonic endoderm fates. *Nature structural & molecular biology*. 2011; 18:120–7.
51. Kuckenber P, et al. The transcription factor TCFAP2C/AP-2gamma cooperates with CDX2 to maintain trophectoderm formation. *Molecular and cellular biology*. 2010; 30:3310–20. [PubMed: 20404091]
52. Chia N-Y, et al. A genome-wide RNAi screen reveals determinants of human embryonic stem cell identity. *Nature*. 2010; 468:316–20. [PubMed: 20953172]

a



b



c

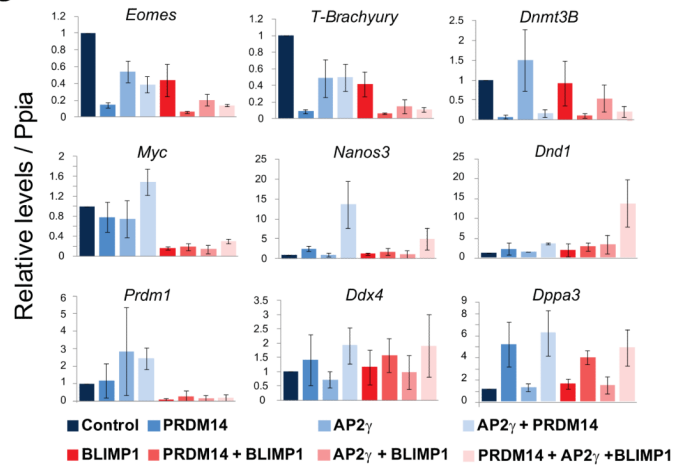


Figure 1. BLIMP1, AP2 and PRDM14 repress somatic regulators and induce PGC genes in P19ECs

(a) Design and overview of the experimental approaches towards transcriptional network for PGC specification. The arrow pointing to PGCs refers to EGFP reporter labelled PGCs in mouse embryos. (b) RT-qPCR analysis of differentially regulated genes downstream of BLIMP1 in P19ECs, showing induction of the PGC genes *Nanos3*, *Rhox9*, *Dppa3*, *Tcfap2c*, *Dnd1*, *Prdm14*, *Dazl* and *Ddx4*. (c) RT-qPCR analysis showing the individual and combinatorial effect of BLIMP1, AP2 and PRDM14 in P19ECs on the mesendodermal transcription factor genes, *Eomes* and *T-Brachyury*, the DNA methyltransferase *Dnmt3b* on

Myc and the PGC genes *Nanos3*, *Dnd1*, *Prdm1*, *Ddx4/Vasa* and *Dppa3*. The error bars in panels (b) and (c) represent standard deviations for 3 independent cell cultures.

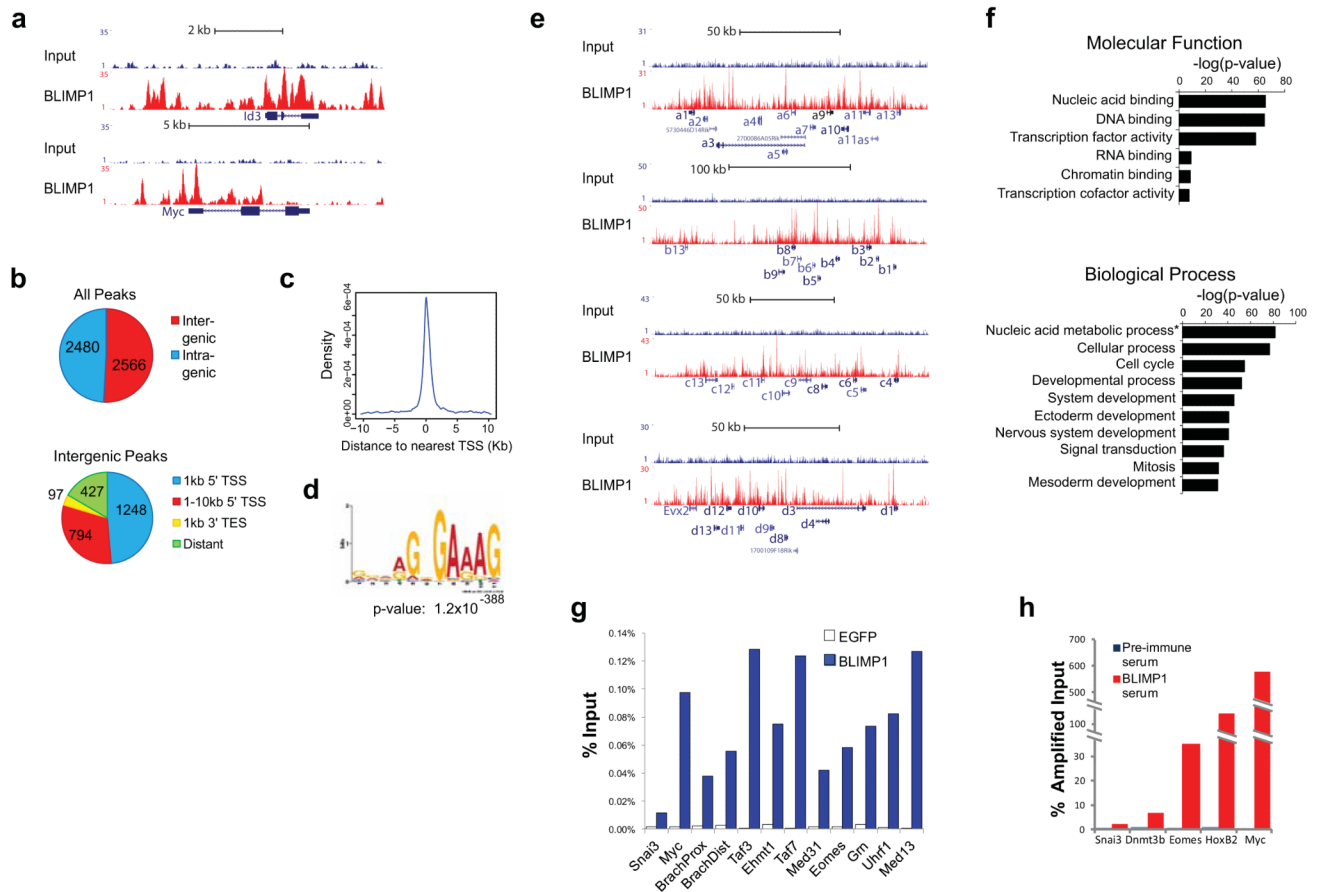


Figure 2. BLIMP1 binding to gene promoters encoding transcription factors, cell cycle and developmental regulators

(a) Track-view of BLIMP1 ChIP-Seq density profile displayed using the UCSC genome browser centred on the *Id3* and *Myc* genes. (b) BLIMP1 peaks distributed roughly evenly between inter- and intragenic positions, with 1248 of 2480 intergenic peaks falling within 1kb 5' of TSS, and 527 peaks were more than 10Kb away from promoters. (TSS: transcriptional start site; TES: transcriptional end site). (c) Distribution of BLIMP1 binding relative to promoters revealing a median distance of +171.5 bp from the TSS. (d) *De novo* motif analysis revealed high enrichment for the BLIMP1 consensus (p-value of 1.2×10^{-388}). (e) BLIMP1 binding profiles on *Hox* gene clusters are indicated in the views with their respective numbers. For example, *Hoxa1* is indicated by a1, *Hoxa2* is a2 and so forth. (f). Functional categories of genes bound by BLIMP1 showing the p-value for the molecular function as well as biological process GO-terms. (g). Validation of novel BLIMP1 binding regions by ChIP-qPCR in P19 EC cells. (h). A validation of novel BLIMP1 binding regions in PGCLCs by ChIP followed by whole genome amplification of precipitated and input DNA assayed by qPCR. The y-axis represents the % of signal from amplified input material at the same starting quantity of the immunoprecipitated DNA to ensure proportional amplification.

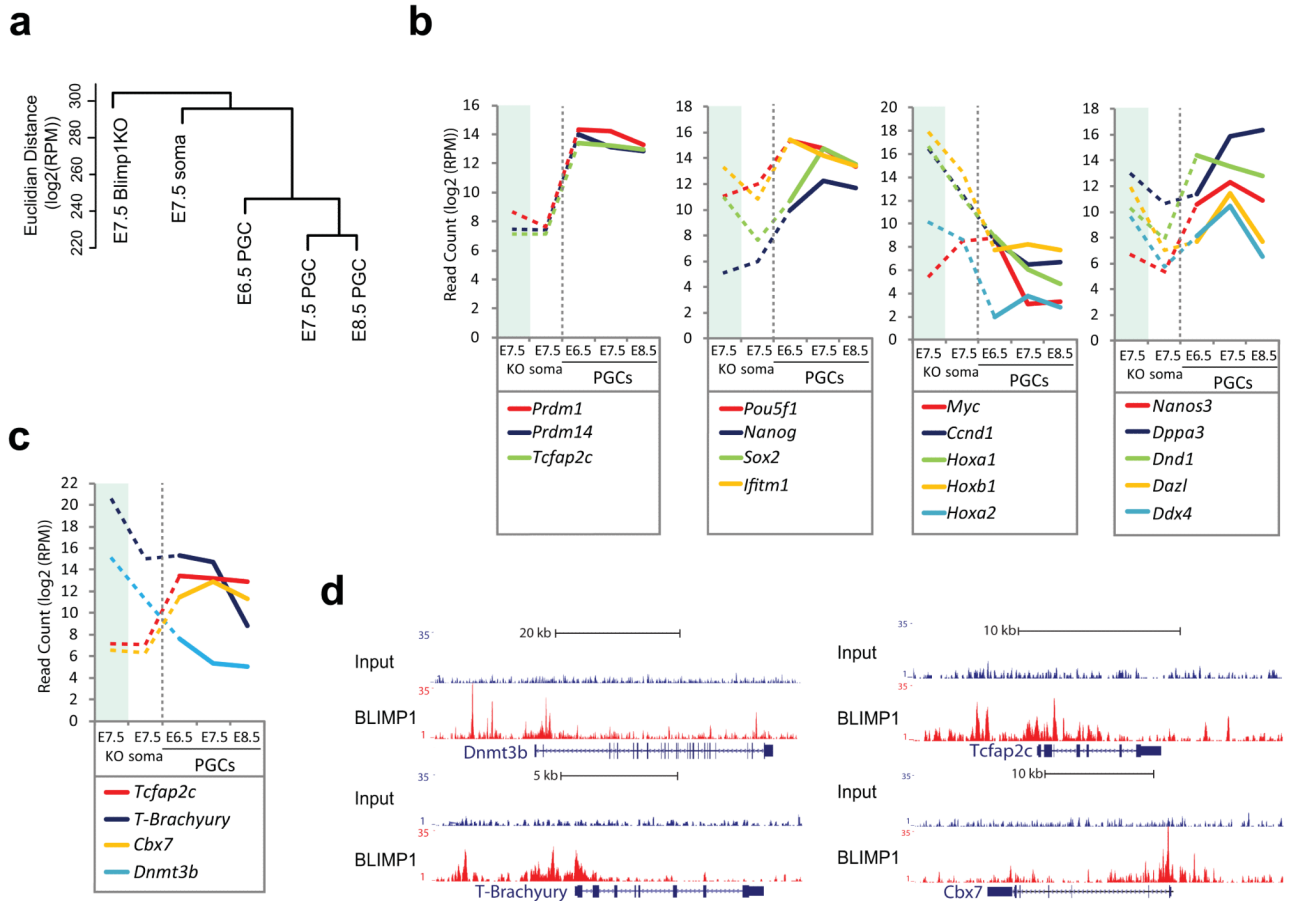


Figure 3. RNA-Seq analysis of PGCs, and BLIMP1 binding to differentially regulated genes (a). Cluster analysis of single-cell RNA-seq expression profiles of PGCs and somatic neighbours. The bar indicates the mean Euclidian distance between the samples. Note that E7.5 BLIMP1 mutant (KO) cells cluster next to E7.5 somatic cells, while the PGCs form distinct clusters following specification (b). Expression levels of selected gene transcripts during PGC specification (RPM=read numbers pr. million reads). The y-axis represents read numbers pr. million reads sequenced. The region shaded in blue represents BLIMP1 mutant (KO) cells. The dotted line represents the onset of PGC specification. (c). Expression of *Dnmt3b*, *T-Brachyury*, *Tcfap2c* and *Cbx7* during PGC specification, which are all bound by BLIMP1 during PGC specification. (d). Track views of BLIMP1 binding to the genomic loci of *Dnmt3b*, *T-Brachyury*, and *Tcfap2c* (encoding AP2) and *Cbx7*.

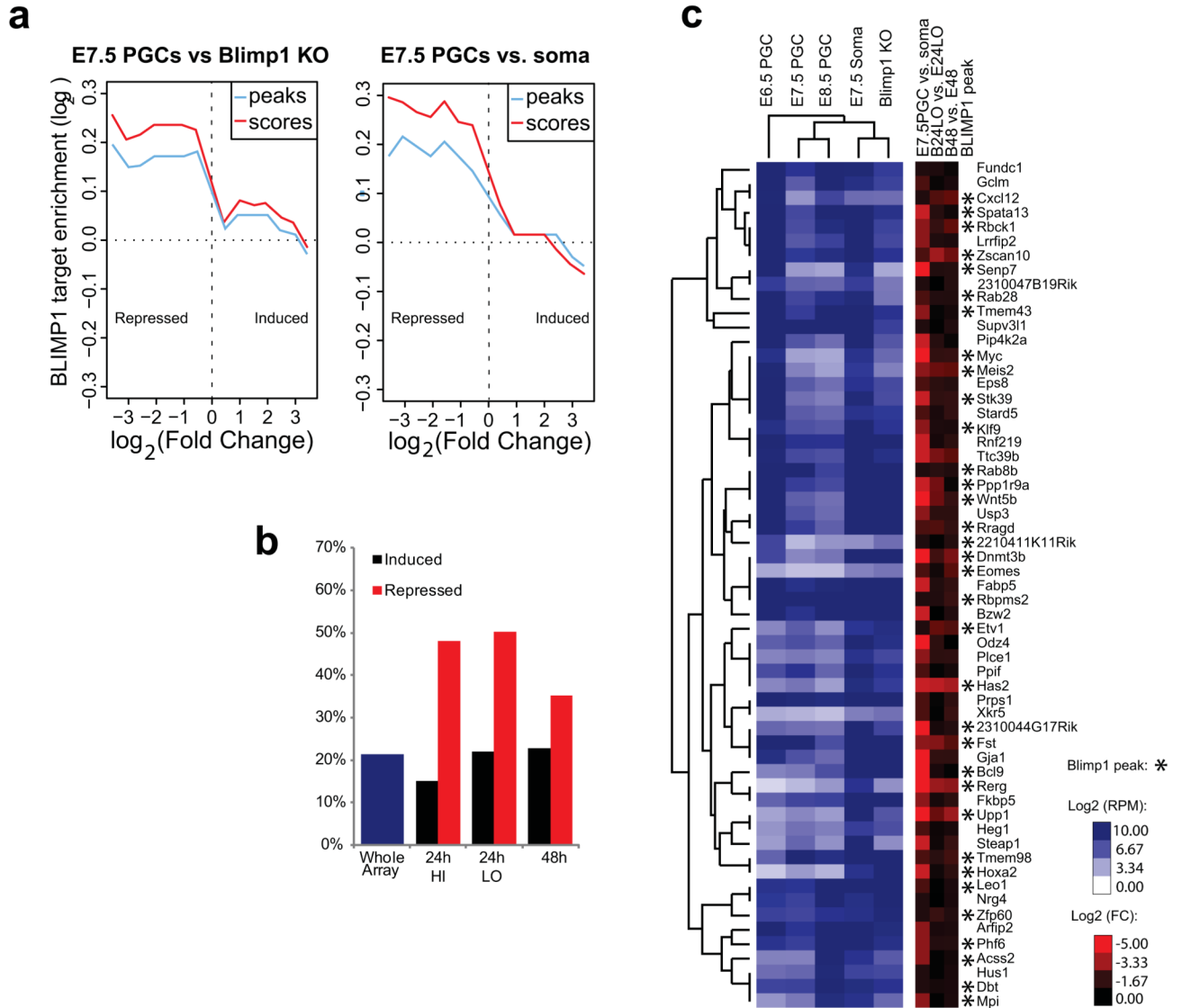


Figure 4. BLIMP1 represses the majority of its direct targets

(a). Relative enrichment of BLIMP1 binding regions and the scores associated with genes differentially expressed between E7.5 PGCs and BLIMP1 mutant (KO) cells, and between E7.5 PGCs and E7.5 somatic cells, respectively. The x-axes indicate the log₂ (fold change) and the y-axes indicate the log₂ of the BLIMP1 target enrichment at each fold change-interval of differentially expressed genes over the average target frequency of the whole expression data set. (Peaks: the enrichment of peaks associated with genes in each interval at E7.5. Scores; the enrichment of binding scores calculated for genes in each interval at E7.5).

(b). Binding frequency of BLIMP1 to genes associated with features on the whole microarray as well as differentially regulated genes (c). Heat map depicting the genes repressed by BLIMP1 in both P19ECs and during PGC specification. The first 4 (blue) columns refer to normalized gene expression levels in PGCs. The next 3 columns (red) reflect values of differential expression between the samples indicated. The asterisks in the final column indicate a high confidence BLIMP1 binding region associated with a gene.

BLIMP1 binding was detected in 34/59 repressed genes in both data sets. (RPM: reads per million. FC: fold change).

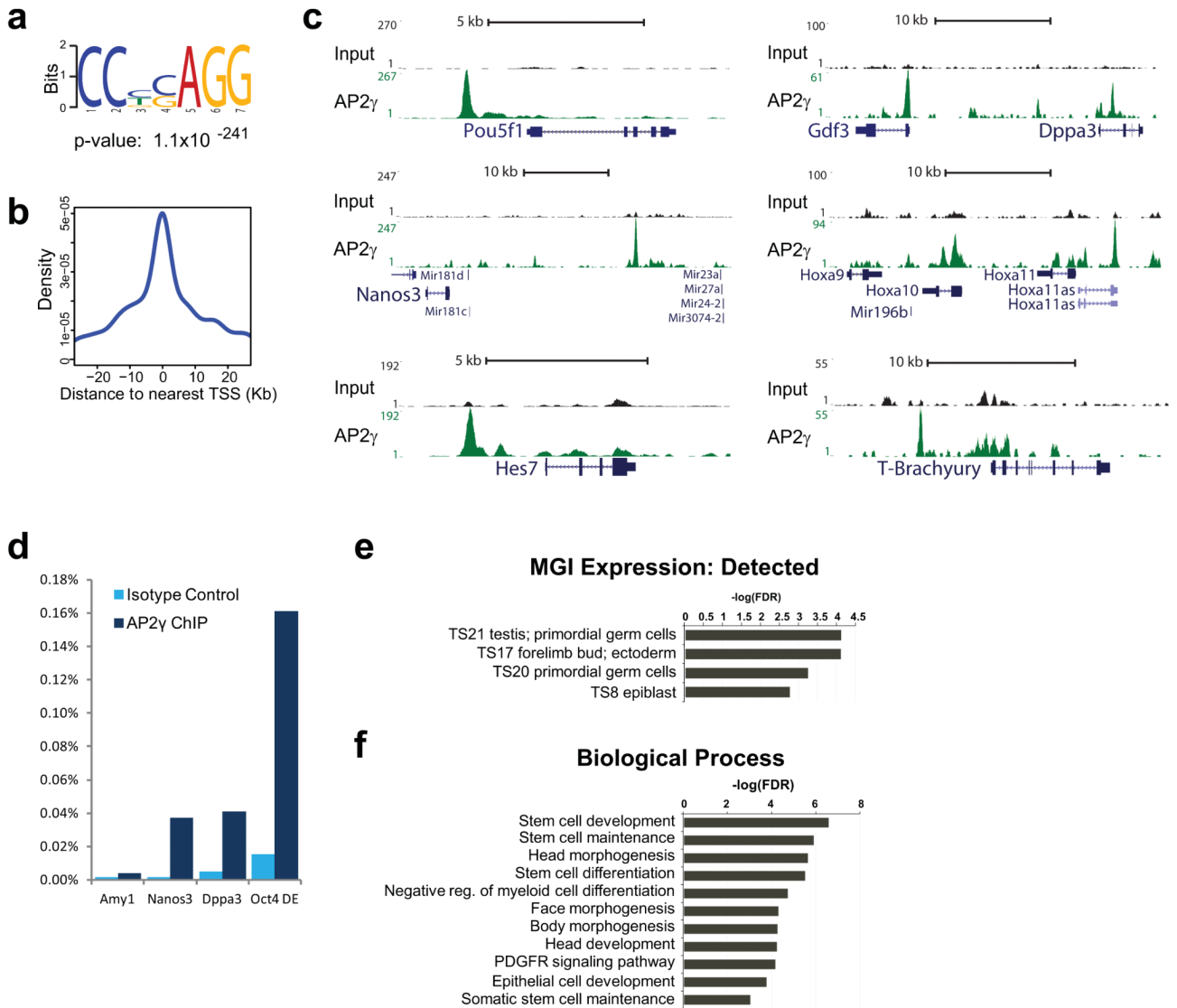


Figure 5. AP2 binds to germ cell genes and somatic regulators

(a). *De novo* motif analysis revealed high enrichment for the AP2 consensus binding site with a p-value of 1.1×10^{-241} . (b). Distribution of AP2 binding relative to promoters revealing a mean distance of +53 bp from the TSS. (c). Track-view of AP2 binding on the *Pou5f1* distal enhancer, to the PGC genes *Dppa3* and *Nanos3*, and the somatic differentiation regulators *HoxA10*, *HoxA11*, *Hes7* and *T-Brachyury*. (d). A ChIP-qPCR of AP2 binding to the promoter of *Nanos3*, *Dppa3/Stella* as well as the distal enhancer of *Oct4* (Oct4-DE). (e). Over represented gene categories sorted by cell-type specific expression at different Theiler Stages (TS) during embryonic development, TS8 corresponds roughly to E6.0, TS17 to E10.5, TS20 to E17 and TS21 to E21/P0. (f). Over represented functional categories of genes bound by AP2 showing the p-value for the enrichment of biological process GO-terms.

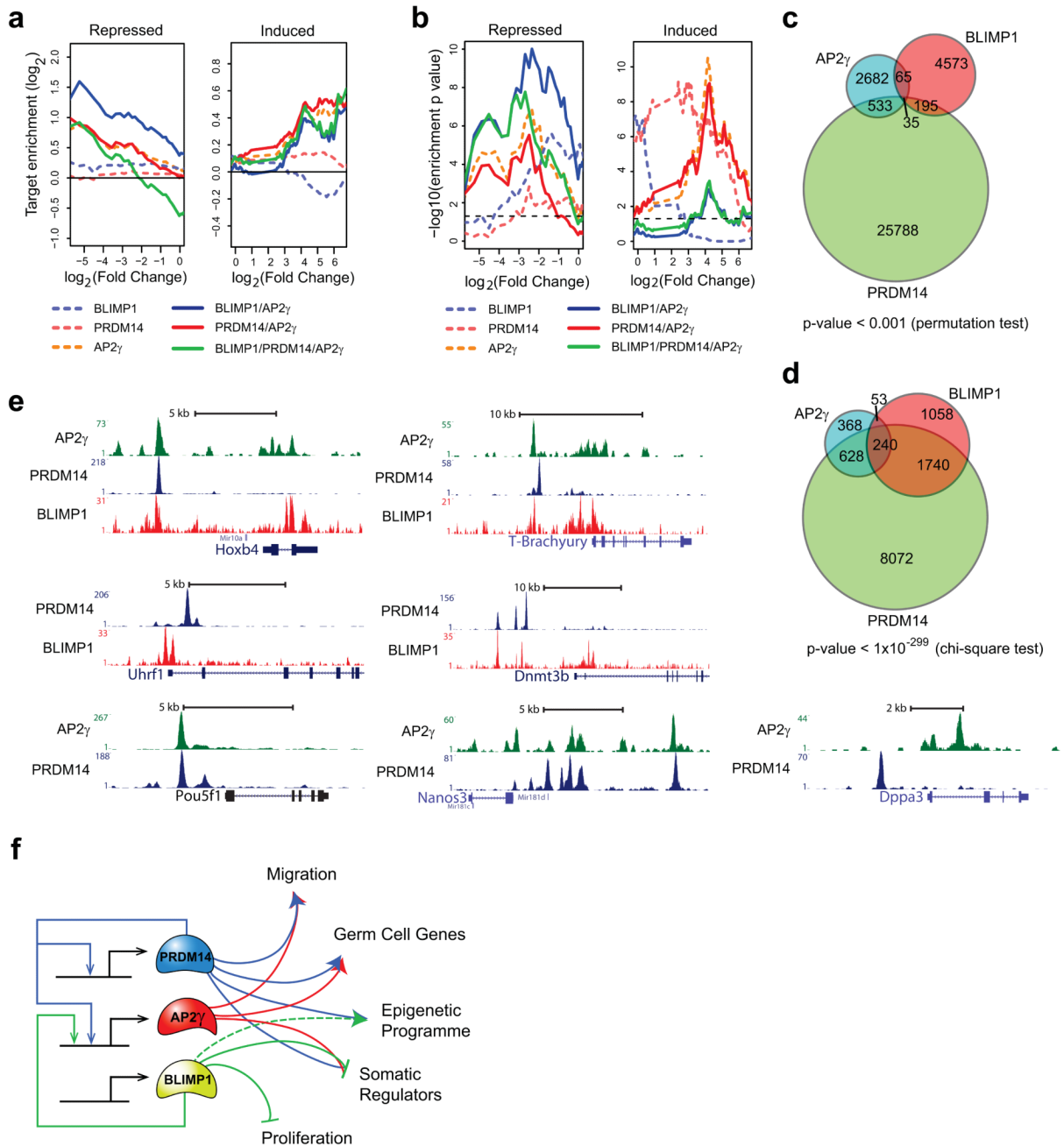


Figure 6. A transcription factor network for PGC specification

(a). Relative enrichment of BLIMP1, AP2 and PRDM14 targets on differentially expressed genes between E7.5 PGCs and soma, and the combinatorial association of the peak regions to the differentially expressed genes. (b). The plots depict the hypergeometric p-values for the corresponding enrichment of BLIMP1, AP2 and Prdm14 targets on differentially expressed genes shown in Fig 6a. (c). Venn diagrams showing the total number of genomic target sites overlapping by one base-pair or more between BLIMP1, AP2 and PRDM14. The p-value for the enrichment of overlap between the factors of $p < 0.0001$ was calculated using a permutation test. See details in Fig. S8a. (d) Venn diagrams showing the total number of genes overlapping between BLIMP1, AP2 and PRDM14. The p-value of $p <$

1×10^{-299} was calculated using a chi-square test. See details in Fig S8b (e). Track-view of BLIMP1, PRDM14 and AP2 binding to selected repressed and induced PGC targets. (f). A transcriptional network model depicting the role of PRDM14, BLIMP1 and AP2 during PGC specification.

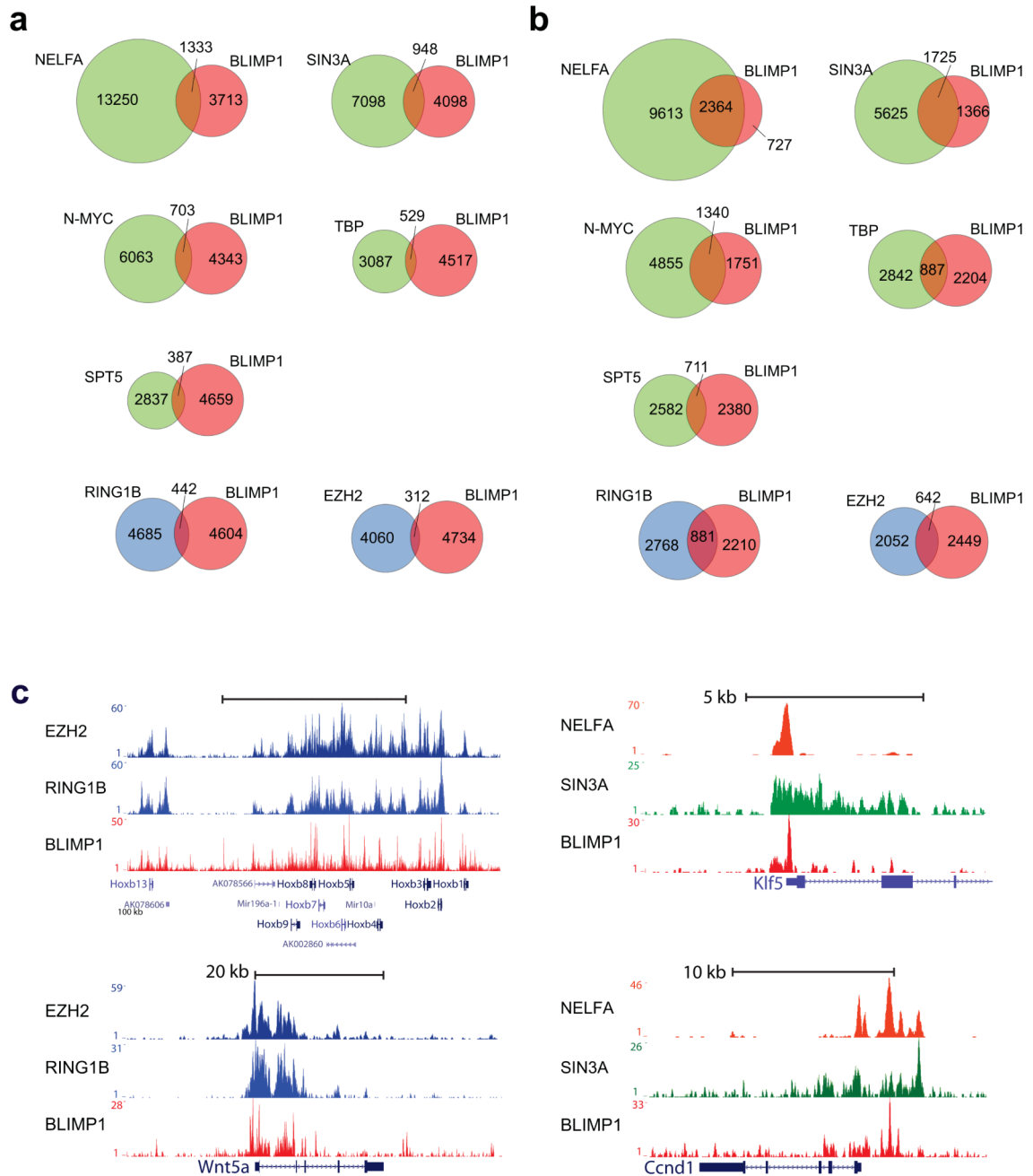


Figure 7. BLIMP1 binds to targets of mESC self-renewal regulators and Polycomb proteins
 (a). Venn diagrams showing the total number of target sites overlapping by one base-pair or more between BLIMP1 on one hand and the indicated transcription factors on the other. (b) Venn diagrams showing the total number of genes overlapping between BLIMP1 on one hand and indicated transcription factors on the other hand. In (a) and (b), the circles for the “self-renewal” cluster genes are indicated in green and the “polycomb” cluster genes in blue
 (c) Track-view of BLIMP1 binding on example genomic loci including the views for EZH2, RING1B, NELFA as well as SIN3A where appropriate.

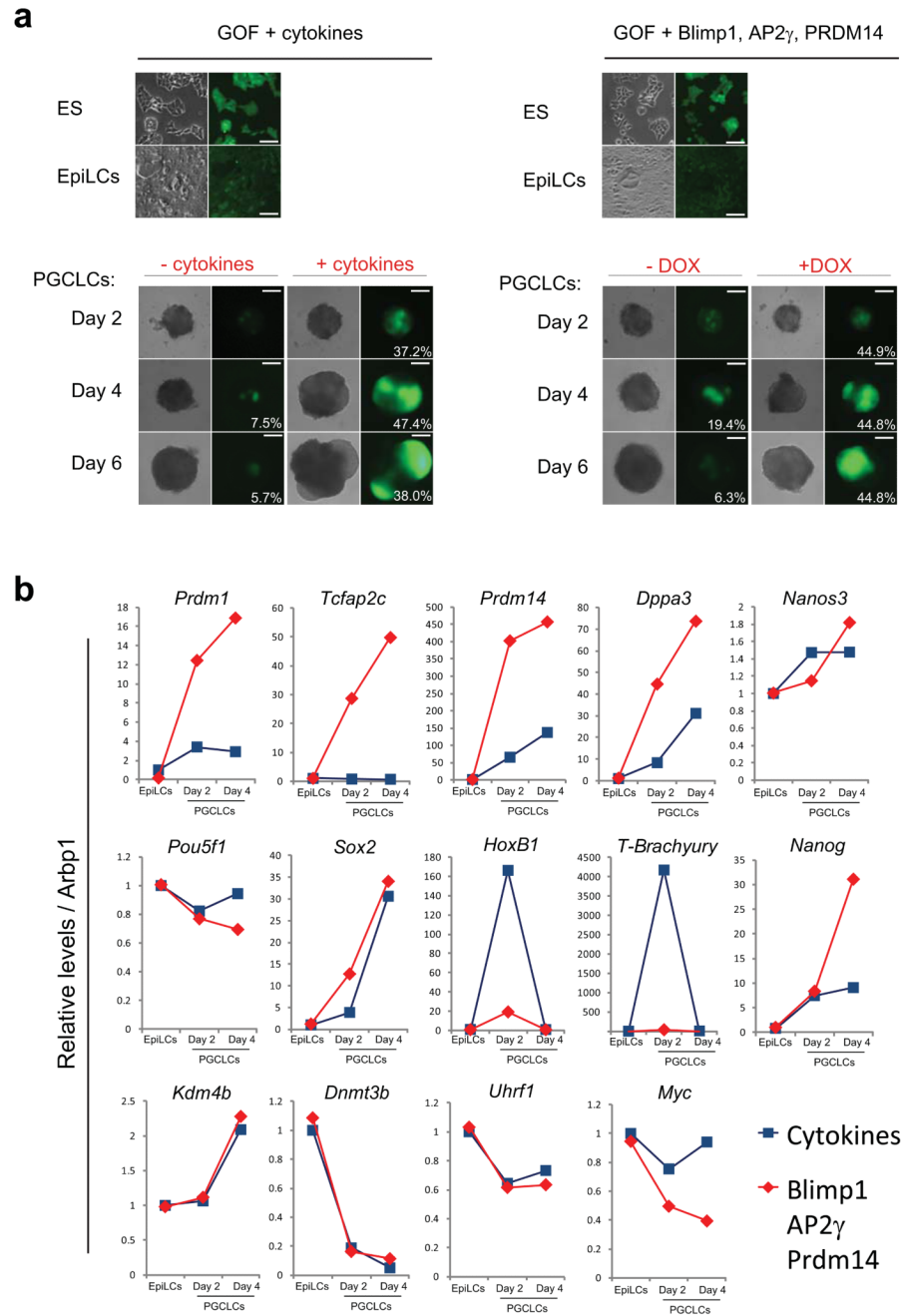


Figure 8. Co-expression of BLIMP1, AP2 and PRDM14 induces PGC-like cell fate *in vitro* (a). Bright-field and fluorescent microscopy images of the Oct4 reporter ESC line (GOF) in culture. The images show ESCs, EpiLCs (stage preceding PGCLC), and PGCLCs as indicated. The left panels show the induction of PGCLCs using cytokines, and the right panels show the induction of PGCLCs without cytokines using doxycycline dependent induction of BLIMP1, AP2 and PRDM14 from GOF cells harbouring stable doxycycline-responsive constructs. The numbers on the figure panels indicate the ratio of fluorescent cells induced at each time-point. (b). RT-qPCR analysis of sorted fluorescent PGCLCs on Day2 and 4 of either cytokine or doxycycline induction, as well as EpiLCs. Panels (a and b) show a representative of two identical experiments.